

CESIUM CHEMISORPTION ONTO STAINLESS STEEL UNDER SIMULATED LIGHT WATER REACTOR SEVERE ACCIDENT

KEMISORPSI CESIUM PADA STAINLESS STEEL DALAM KONDISI SIMULASI KECELAKAAN PARAH REAKTOR NUKLIR BERPENDINGIN AIR RINGAN

I Wayan Ngarayana^{1,*}

¹Research Center for Nuclear Technology, Research Organization for Nuclear Energy, National Research and Innovation Agency, BJ Habibie Integrated Science Area Building No. 80 Serpong, Tangerang Selatan 15312, Indonesia

*Corresponding author e-mail: iway018@brin.go.id

Received 8 February 2023, revised 31 March 2023, accepted 19 June 2023

ABSTRACT

CESIUM CHEMISORPTION ONTO STAINLESS STEEL UNDER SIMULATED LIGHT WATER REACTOR SEVERE ACCIDENT. This study investigates the interactions between cesium and stainless-steel structural materials under simulated light water reactor severe accident conditions. Cesium is a major source term that can form new compounds with structural materials and affect their volatility, leading to late release of radioactivity. Existing codes cannot accurately estimate this phenomenon. Previous studies have predicted the physicochemical interactions between cesium and structural materials, but the types of chemisorbed cesium compounds are still unclear. This study uses advanced techniques, such as SEM/EDS, and TEM, to identify the chemisorbed cesium compounds on the oxide layer of stainless steel. The results suggest that cesium is strongly absorbed in the form of cesium silica, cesium aluminum silica, and/or cesium ferro silica, with CsFeSiO_4 and CsAlSiO_4 being the dominant compounds. However, these compounds share the same crystal structure, which makes it challenging to distinguish them using the utilized technique.

Keywords: Cesium, source terms, chemisorption, stainless steel, SEM, TEM, FIB.

ABSTRAK

KEMISORPSI CESIUM PADA STAINLESS STEEL DALAM KONDISI SIMULASI KECELAKAAN PARAH REAKTOR NUKLIR BERPENDINGIN AIR RINGAN. Studi ini menyelidiki interaksi antara cesium dan bahan struktur baja tahan karat di bawah simulasi kondisi kecelakaan parah reaktor air ringan. Cesium adalah source term utama yang dapat membentuk senyawa baru dengan bahan struktural dan memengaruhi volatilitasnya, yang menyebabkan late release radioaktivitas. Kode yang ada belum dapat secara akurat memperkirakan fenomena ini. Studi sebelumnya telah memperkirakan interaksi fisikokimia antara cesium dan bahan struktural, tetapi jenis senyawa cesium yang terkemisorpsi masih belum jelas. Studi ini menggunakan teknik maju, terutama SEM/EDS dan TEM, untuk mengidentifikasi senyawa cesium yang terkemisorpsi pada lapisan oksida baja tahan karat. Hasilnya menunjukkan bahwa cesium terabsorpsi kuat dalam bentuk cesium silika, cesium aluminium silika, dan/atau cesium ferro silika, dengan CsFeSiO_4 dan CsAlSiO_4 menjadi senyawa yang dominan. Namun, senyawa ini memiliki struktur kristal yang sama, sehingga sulit untuk membedakannya menggunakan teknik yang digunakan.

Kata kunci: Cesium, source terms, kemisorpsi, stainless steel, SEM, TEM, FIB.

INTRODUCTION

Cesium (Cs) chemisorption is a crucial phenomenon that affects the accuracy of estimating the source terms released into the environment during a nuclear reactor severe accident [1]–[5]. Cs may be released from the degraded core and transported through the leakage parts under high temperature conditions [6]–[8]. Cs may react with structural materials through various mechanisms involving gas-solid and liquid-solid reactions [9]–[11]. The types of Cs compounds formed depend on the types of Cs species, structural materials, temperature, and environmental conditions. Cesium ferrate (Cs-Fe-O) and cesium chromate (Cs-Cr-O) are commonly formed, but they are easily dissolved by water [12], [13]. Other types of Cs compounds, such as cesium silicate (Cs-Si-O) and cesium ferro silicate (Cs-Fe-Si-O), are predicted to be strongly chemisorbed onto the material matrix [14]–[17]. A better understanding of the species and physiochemistry of chemisorbed Cs is required for developing databases to improve the source terms codes [18]–[20].

However, the physiochemistry of chemisorbed Cs remains unclear despite many experimental studies. The types of chemisorbed Cs species formed on structural materials are also controversial. Therefore, this study simulated chemisorbed Cs on stainless steel (SS) 304, which is one of the main structural materials in light water reactors (LWRs). The chemisorbed Cs was analyzed using advanced techniques, such as scanning electron microscope (SEM) and transmission electron microscope (TEM) with energy dispersive x-ray spectroscopy (EDS) and assisted by focus ion beam (FIB) for sample preparation.

METHODOLOGY

SPECIMEN TREATMENT

Received Specimens

Cesium hydroxide monohydrate ($\text{CsOH}\cdot\text{H}_2\text{O}$) provided by Combi-Blocks Inc. was utilized as the precursor. The utilized Cs precursor has around 95% purity and was identified to have a P3m1 space group which matches the database of the international center for diffraction data number 00-036-0771 [12].

Stainless steel (SS) 304 specimen with the elemental composition shown in Table 1 was obtained from Nilaco Corporation and used to simulate the structural material. The specimen was cut into 10 mm × 10 mm × 5 mm samples using a low speed cutting machine. The samples were polished with silicon carbide papers of 0-, 30-, 15-, 10-, and 5- μm grit sizes and then with diamond and alumina suspensions of 3- μm and 0.05- μm particle sizes, respectively.

Table 1. Elemental concentration (wt.%) of received SS 304

| Elements | Fe | Cr | Ni | Mn | Si | Al |
|---------------------------|---------|-------|------|------|------|------|
| Published by manufacturer | balance | 17-19 | 8-11 | ≤ 2 | ≤ 1 | - |
| Measured by EDS | 71.19 | 18.34 | 7.98 | 0.97 | 0.41 | 0.45 |

Specimens Preparation

Specimen preparation followed the previous studies by Japan Atomic Energy Agency (JAEA) [11]. The experimental apparatus in Figure 1 simulated the LWR severe accident. $\text{CsOH}\cdot\text{H}_2\text{O}$ precursor was heated to 650 °C and transported to the SS 304 target specimen by a gas flow of 100 mL/min consisting of argon gas and about 5% of water steam (H_2O). Argon gas is used to simulate the reducing conditions that may occur in the reactor coolant system under high temperature and hydrogen production [21]. The target specimen was maintained at 1000 °C for 6 hours and then cooled down to room temperature for 3 hours. To account for possible water vapor condensation after exposure, the specimen was immersed in 20 mL water at room temperature for 1 day.

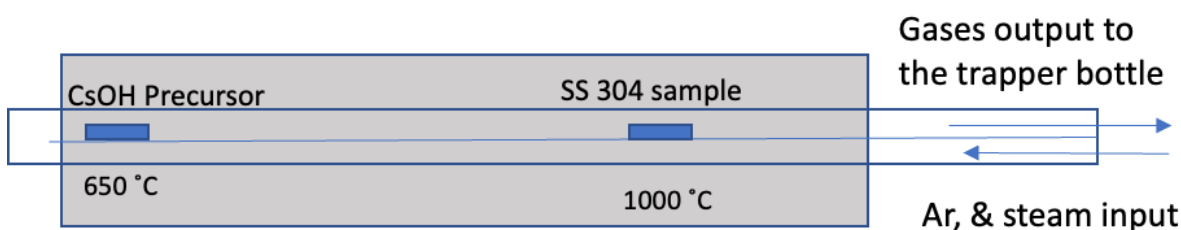


Figure 1. Schematic setup of the experimental apparatus to simulate LWR severe accident

Characterization

The surface morphology and elemental distribution were analyzed using an SEM Jeol JCM-6000Plus with EDS and embedded software that performed quantitative analysis using the atomic number, absorption, and fluorescence (ZAF) correction method with a detection limit of 0.15 at.%. The SEM operated at 15 kV acceleration voltage and 7.475 nA irradiation current in a high vacuum environment.

For more detailed observations, a TEM Hitachi HT7700 with high-resolution EDS was used to produce electron diffraction that indicated the crystal structure of the compounds. The TEM operated at 100 kV acceleration voltage and 12.6 μA irradiation current.

The TEM specimens were prepared using FIB 2200 by Hitachi. The specimens were protected by tungsten (W) deposition and cut by gallium (Ga) ion sources during fabrication.

RESULTS AND DISCUSSIONS

SEM/EDS OBSERVATION

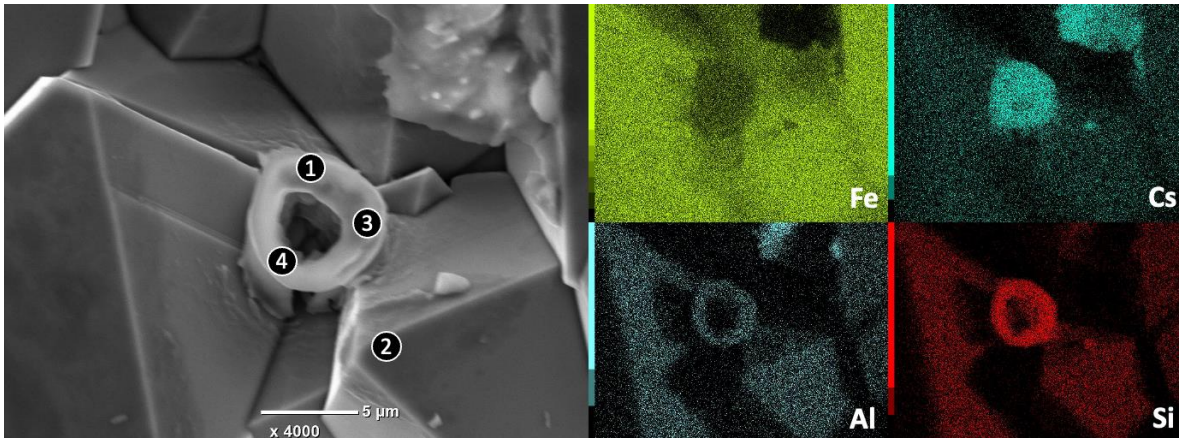


Figure 2. SEM/EDS analysis of the specimen surface showing the formation of Cs-Si-Al-O compounds as circular deposits

Figure 2 shows the SEM observation of the surface, where circular deposits of Cs are visible between chunks. Other forms of Cs deposits were also observed, but they had lower concentrations of Cs than the circular ones. The EDS mapping revealed that the circular deposits were composed of Cs, Si, Al, and O. Table 2 presents the results of the EDS point analysis on the circular deposits and the surrounding area. The circular deposits had higher concentrations of Cs, Si, and Al than the surrounding area, while other elements did not show significant differences.

Table 2. EDS point analysis of selected areas in Figure 2, showing that the circular deposit is a cesium compound associated with O, Al, and Si

| Elements | Atomic concentration (at.%) of point: | | | | |
|----------|---------------------------------------|-------|-------|-------|-------|
| | 1 | 2 | 3 | 4 | 5 |
| O | 58.54 | 53.77 | 66.2 | 65.6 | 58.54 |
| Al | 0.92 | 0.51 | 0.75 | 0.79 | 0.92 |
| Si | 6.55 | 0.07 | 5.81 | 5.77 | 6.55 |
| Cr | 0.22 | 0.93 | 0.17 | 0.12 | 0.22 |
| Mn | 0.32 | 0.91 | 0.22 | 0.26 | 0.32 |
| Fe | 24.79 | 43.71 | 20.75 | 20.86 | 24.79 |
| Ni | 0 | 0.01 | 0 | 0 | 0 |
| Cs | 8.63 | 0.09 | 6.01 | 6.52 | 8.63 |

The average concentrations of Cs, Si, Al, and O in the circular deposits, based on several repeated measurements, were about: 7.05 ± 0.80 at.%, 6.04 ± 0.25 at.%, 0.823 ± 0.11 at.%, and 63.45 ± 2.46 at.%, respectively. These values suggest that the circular deposits could be cesium silicate (Cs-Si-O), cesium aluminate (Cs-Al-O), cesium aluminosilicate (Cs-Al-Si-O), or even cesium ferrisilicate (Cs-Fe-Si-O) due to the high Fe content. However, SEM/EDS analysis is not sufficient to identify the exact compound type. Therefore, further characterization methods are needed.

TEM OBSERVATION

FIB is the only method that can be used to prepare TEM samples from objects smaller than 5 μm . This is also the most challenging step in this study.

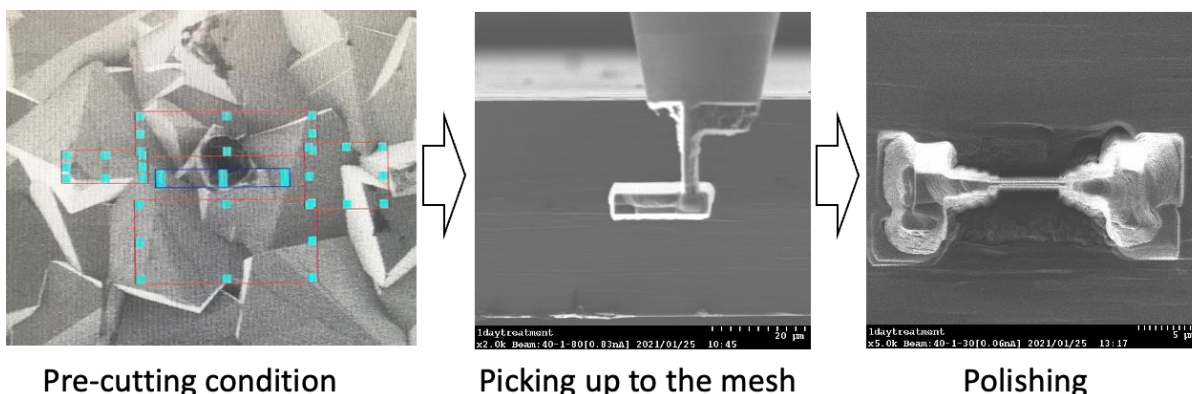


Figure 3. TEM sample preparation using FIB on the circular deposits identified by SEM/EDS

Figure 3 shows the TEM sample preparation using FIB based on the SEM/EDS observations. The target deposit was first coated with tungsten to protect it from damage during the cutting process. Then, the sample was cut to about 6 μm and transferred to a suitable mesh. Finally, the sample on the mesh was thinned and polished until it reached a thickness of less than 80 nm.

Figure 4 shows the TEM/EDS cross-section of the circular deposit indicated in Figure 2. The EDS mapping and point analysis in Table 3 reveal that the dark areas on the top part (right image) are due to the probe and W deposition. The lower part of the target area (red circle) is likely an oxide layer, mainly composed of iron oxides. Cu was also detected in almost all parts of the sample, because the mesh used was made of Cu. Cu and W atoms were scattered and deposited on the sample during the cutting and polishing process. Therefore, Cu and W can be ignored in these data.

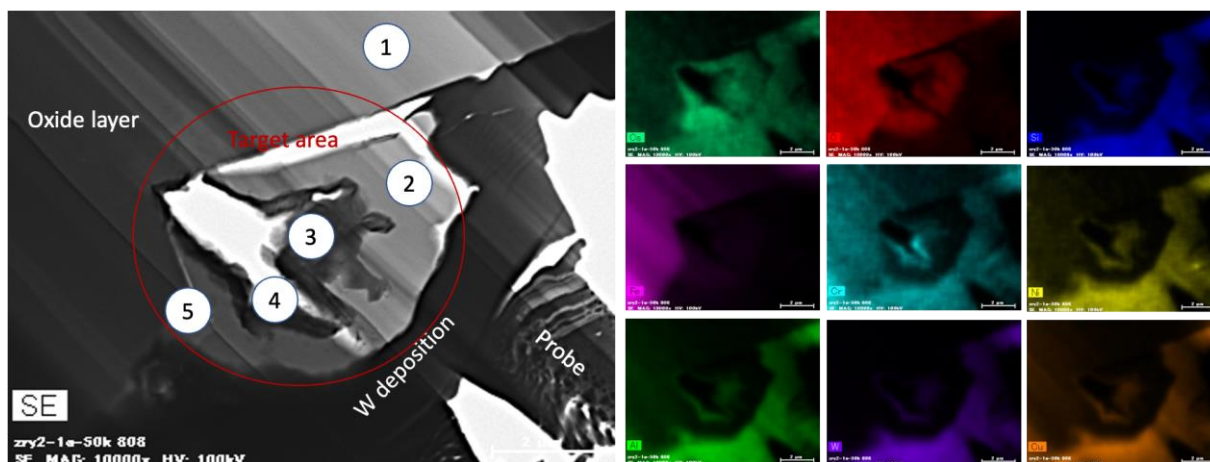


Figure 4. TEM/EDS cross-section of the sample showing the Cs-rich region in the red circle

The TEM/EDS observations confirm the SEM/EDS results. The EDS elemental mapping and point analysis show that Cs is associated with Si and Al. This supports the hypothesis that the chemisorbed Cs on the structural material forms Cs-Si-O, Cs-Al-O, Cs-Al-Si-O, and/or Cs-Fe-Si-O compounds.

To obtain a more accurate prediction of compound species, we attempted to observe the important data from TEM, namely electron diffraction patterns, d-spacing, and orientation between atoms, as shown in Figure 5. Unfortunately, important data related to Cs was very difficult to observe. This is because as shown in Table 3, the concentration of Cs in the structure was relatively low, less than 10 at.%. Although the bright areas in area (2) contained around 5.37 at.% of Cs, data shown in Figure 5 indicated the domination of iron oxides, especially Fe_2O_3 . The darker area, namely in area (3), which contained around 9.23 at.% of Cs, showed a slightly different electron diffraction pattern and atomic d-spacing. Although it could not provide predictions with high confidence, crystal structures in that area might be related to CsFeSiO_4 , which had an orthorhombic crystal system and Pna2₁ space group [22]. Except for its size, CsAlSiO_4 also had the same crystal structure as CsFeSiO_4 [22]. So, considering the

presence of around 5.61 at.% Al in the area, it was possible that the area was also composed of CsAlSiO_4 compounds.

Table 3. EDS point analysis of selected regions in Figure 4 shows that Cs is associated with Si and Al

| Elements | Atomic concentration (at.%) of point: | | | | |
|----------|---------------------------------------|-------|-------|-------|-------|
| | 1 | 2 | 3 | 4 | 5 |
| O | 36.22 | 48.36 | 17.61 | 19.14 | 20.32 |
| Al | 0.30 | 3.19 | 5.61 | 0.82 | 1.61 |
| Si | 0.09 | 6.47 | 7.48 | 1.23 | 2.01 |
| Cr | 0.99 | 0 | 0.02 | 7.15 | 0.23 |
| Fe | 52.02 | 27.69 | 46.04 | 34.89 | 22.35 |
| Ni | 0.28 | 0 | 0 | 2.41 | 0.22 |
| Cu | 7.60 | 8.51 | 12.92 | 18.67 | 36.10 |
| Cs | 0 | 5.37 | 9.23 | 2.42 | 3.02 |
| W | 0.25 | 0.37 | 1.10 | 3.72 | 17.32 |

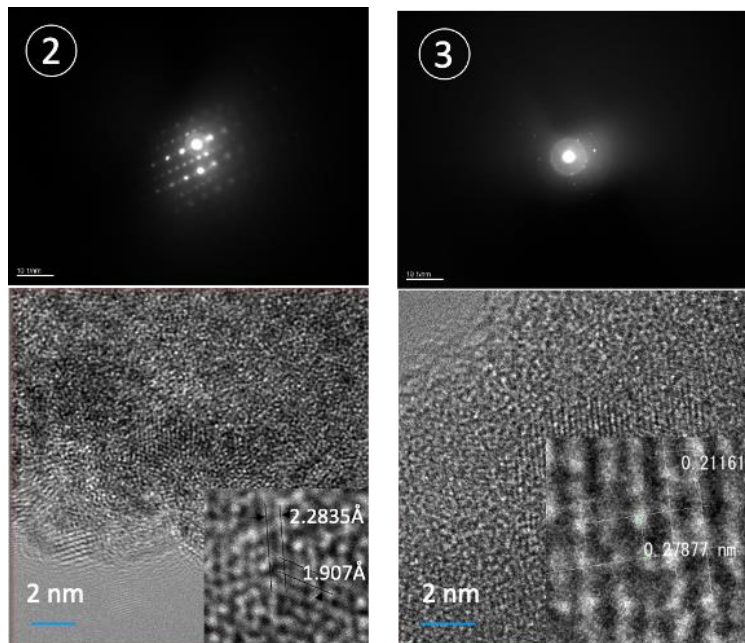


Figure 5. Electron diffraction and high-resolution TEM images of areas (2) and (3) as shown in Fig. 4. Electron diffraction and d-spacing of areas (2) and (3) were closely related to Fe_2O_4 and CsFeSiO_4 , respectively

CONCLUSION

This research was conducted to identify the type of Cs compound absorbed into the structural material of SS 304 by simulating LWR severe accident. The structure of the chemisorbed Cs was observed using SEM and TEM equipped with EDS and assisted by the FIB machine in sample preparation. Both surface SEM/EDS and cross-sectional TEM/EDS observations provided a strong indication of the presence of cesium silica, cesium alumina, cesium alumina silica, and/or cesium ferro silica compounds. The exact species of the compound was expected to be determined based on electron diffraction, atomic distance and orientation from TEM data. Unfortunately, due to the low concentrations of Cs, as well as Si and Al, data related to the crystal structure of these

compounds was very difficult to find. Nonetheless, from the obtained data, the chemisorbed Cs-enriched circle-shaped object onto SS 304 structural material might be related to CsFeSiO₄ and CsAlSiO₄. However, both structures had similar crystal systems that made them difficult to identify with certainty in this study.

ACKNOWLEDGMENTS

This work was supported by the Radioisotope Center and the Extreme Energy-Density Research Institute of Nagaoka University of Technology, who provided us with the TEM, SEM/EDS and FIB machines that we used in this study. We also thank JAEA for providing us with valuable information and specimens. Additionally, part of this study was funded by the RIIM3 project.

REFERENCES

- [1] K. Nakajima, E. Suzuki, N. Miyahara, and M. Osaka, "An experimental investigation for atmospheric effects on Cs chemisorption onto stainless steel," *Progress in Nuclear Science and Technology*, vol. 5, no. 0, pp. 168–170, 2018, doi: 10.15669/pnst.5.168.
- [2] F. G. Di Lemma, K. Nakajima, S. Yamashita, and M. Osaka, "Experimental investigation of the influence of Mo contained in stainless steel on Cs chemisorption behavior," *Journal of Nuclear Materials*, vol. 484, pp. 174–182, Feb. 2017, doi: 10.1016/j.jnucmat.2016.11.031.
- [3] K. K. Nabaichuan Li, K. Nakajima, E. Suzuki, "Study and evaluation of cesium chemisorption behavior onto steel under simulated nuclear reactor severe accident environment in 400°C," in *AESJ Fall Meeting 2021*, AESJ, 2021, p. 3E04.
- [4] M. Osaka, M. Gouëlo, and K. Nakajima, "Cesium Chemistry in the LWR severe accident and towards the decommissioning of Fukushima Daiichi Nuclear Power Station," *Journal of Nuclear Science and Technology*, vol. 59, no. 3, pp. 292–305, Mar. 2022, doi: 10.1080/00223131.2021.1997664.
- [5] S. Nichenko, J. Kalilainen, L. F. Moguel, and T. Lind, "Modelling of fission products release in VERDON-1 experiment with cGEMS: Coupling of severe accident code MELCOR with GEMS thermodynamic modelling package," *Annals of Nuclear Energy*, vol. 152, p. 107972, 2021, doi: 10.1016/j.anucene.2020.107972.
- [6] A. Watanabe, K. Yamada, and M. Ohsaki, "FP Aerosol Trapping Effect Along the Leakage Paths of Degraded Containment Penetrations During a Severe Accident (II) Decontamination Factor at the Containment Penetrations and Its Application to Actual Plant," *Transactions of the Atomic Energy Society of Japan*, vol. 8, no. 4, pp. 332–343, 2009, doi: 10.3327/taesj.J08.052.
- [7] M. Firnhaber, T. F. Kanzleiter, S. Schwarz, and G. Weber, "International Standard Problem ISP37: VANAM M3. A Multicompartment Aerosol Depletion Test with Hygroscopic Aerosol Material," *Committee on the Safety of Nuclear Installations OECD Nuclear Energy Agency*, Moulineaux, 1996.
- [8] S. Gupta, "Experimental investigations relevant for hydrogen and fission product issues raised by the Fukushima accident," *Nuclear Engineering and Technology*, vol. 47, no. 1, pp. 11–25, 2015, doi: 10.1016/j.net.2015.01.002.
- [9] D. Cubicciotti and B. R. Sehgal, "Vapor Transport of Fission Products in Postulated Severe Light Water Reactor Accidents," *Nuclear Technology*, pp. 266–291, 1984, doi: <https://doi.org/10.13182/NT84-A33411>.
- [10] P. Szajerski, A. Bogobowicz, and A. Gasiorowski, "Cesium retention and release from sulfur polymer concrete matrix under normal and accidental conditions," *Journal of Hazardous Materials*, vol. 381, no. February 2019, p. 121180, 2020, doi: 10.1016/j.jhazmat.2019.121180.
- [11] Miradji, F., et al., "Modelling of Cesium Chemisorption Under Nuclear Power Plant Severe Accident Conditions," in *The 9TH European Review Meeting on Severe Accident Research (ERMSAR2019)*, Prague, 2019.
- [12] I. W. Ngarayana, K. Murakami, and T. M. D. Do, "Effect of surface oxidation on the cesium chemisorption behavior of SS 304, Inconel 600 and X-750," *Journal of Nuclear Science and Technology*, pp. 1–11, Feb. 2022, doi: 10.1080/00223131.2022.2029608.
- [13] I. W. Ngarayana, K. Murakami, T. Suzuki, and T. M. D. Do, "Role of solute titanium and oxidation in cesium chemisorption onto stainless steel," *Journal of Nuclear Science and Technology*, p. 10, 2022, doi: <https://doi.org/10.1080/00223131.2022.2134225>.

- [14] C. Suzuki, K. Nakajima, and M. Osaka, "Phase stability of Cs-Si-O and Cs-Si-Fe-O compounds on stainless steel," *Journal of Nuclear Science and Technology*, pp. 1–12, Oct. 2021, doi: 10.1080/00223131.2021.1971576.
- [15] G. C. Allen, B. R. Bowsher, S. Dickinson, G. M. Fotios, A. L. Nichols, and R. K. Wild, "Surface studies of the interaction of cesium hydroxide vapor with 304 stainless steel," *Oxidation of Metals*, vol. 28, no. 1–2, pp. 33–59, 1987, doi: 10.1007/BF00666470.
- [16] R. Elrick, R. Sallach, A. Oulette, and S. Douglas, "Reaction between some Cesium-Iodine compounds and the reactors materials 304 stainless steel, Inconel 600 and Silver, Volume I Cesium Hydroxide Reactions," US NRC, Albuquerque, NM (USA), 1984.
- [17] K. Nakajima, S. Nishioka, E. Suzuki, and M. Osaka, "Study on chemisorption model of cesium hydroxide onto stainless steel type 304," *International Conference on Nuclear Engineering, Proceedings, ICONE*, vol. 2019-May, 2019, doi: 10.1299/mej.19-00564.
- [18] JAEA, "Fission Product Chemistry Database ECUME Version 1.1," Japan Atomic Energy Agency, Tokai-mura, 2019. doi: 10.11484/jaea-data-code-2019-017.
- [19] N. Miyahara, S. Miwa, N. Horiguchi, I. Sato, and O. Masahiko, "Chemical reaction kinetics dataset of Cs-I-B-Mo-O-H system for evaluation of fission product chemistry under LWR severe accident conditions," *Journal of Nuclear Science and Technology*, vol. 56, no. 2, pp. 228–240, 2019, doi: 10.1080/00223131.2018.1544939.
- [20] M. Osaka, et al., "Results and Progress of Fundamental Research on Fission Product Chemistry - Progress Report in 2015," Japan Atomic Energy Agency, Tokai-mura, 2016. doi: 10.11484/jaea-review-2016-026.
- [21] N. Miyahara, et al., "Experimental study on transport behavior of cesium iodide in the reactor coolant system under LWR severe accident conditions," *Journal of Nuclear Science and Technology*, vol. 57, no. 12, pp. 1287–1296, Dec. 2020, doi: 10.1080/00223131.2020.1782281.
- [22] A. Jain, et al., "Commentary: The Materials Project: A materials genome approach to accelerating materials innovation," *APL Materials*, vol. 1, no. 1, p. 011002, Jul. 2013, doi: 10.1063/1.4812323.